

NASA TECHNICAL NOTE



NASA TN D-2819

NASA TN D-2819

FACILITY FORM 602

N65-24377
(ACCESSION NUMBER)

12
(PAGES)

(NASA CR OR TMX OR AD NUMBER)

THRU

(CODE)

15
(CATEGORY)

DEVELOPMENT OF A SEALED BRUSHLESS DC MOTOR

by Philip A. Studer

*Goddard Space Flight Center
Greenbelt, Md.*

GPO PRICE \$ _____

OTS PRICE(S) \$ 1.00

Hard copy (HC) _____

Microfiche (MF) 150

DEVELOPMENT OF A SEALED BRUSHLESS DC MOTOR

By Philip A. Studer

Goddard Space Flight Center
Greenbelt, Md.

NATIONAL AERONAUTICS AND SPACE ADMINISTRATION

For sale by the Clearinghouse for Federal Scientific and Technical Information
Springfield, Virginia 22151 - Price \$1.00

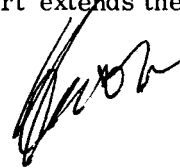
DEVELOPMENT OF A SEALED BRUSHLESS DC MOTOR

by
Philip A. Studer
Goddard Space Flight Center

SUMMARY

24377

Sealed "brushless" d.c. instrument motors for space application have achieved performance levels that indicate no size or efficiency penalty remains, while increased independence of the environment is secured through photo-electronic commutation. The motors reach efficiencies of 65%. A typical unit develops 0.25 in.-oz. of torque at 3000 rpm with a power input of one watt. A stall torque of 3.25 in.-oz. reduces the mechanical time constant to an extremely low value. The predicted reliability for one year of continuous operation is 94.4%. Sealing of the windings and electronics prevents outgassing from affecting nearby sensitive instrumentation. This type of motor should be considered for space applications where high torque, efficiency and reliability as well as minimal outgassing are important factors. This report extends the work reported earlier in NASA Technical Note D-2108.



CONTENTS

Summary	iii
INTRODUCTION	1
EFFICIENCY	3
RELIABILITY	4
HERMETIC SEALING	5
SIZE REDUCTION	6
PERFORMANCE	7
CONCLUSION	7
References	8

DEVELOPMENT OF A SEALED BRUSHLESS DC MOTOR

by

Philip A. Studer

Goddard Space Flight Center

INTRODUCTION

This report describes the recent developments in a brushless dc motor program. The program objectives were to increase the efficiency and reliability of the device while reducing its size. The program included the development of a hermetically sealed motor which could be used in vacuum chambers or space applications where outgassing of organic vapors was objectionable.

The feasibility of the brushless motor concept and a practical device have been reported earlier (Reference 1). The concept of electronic commutation itself had been developed to provide the characteristics of a true dc motor for operation in high vacuum. Safe operation in hazardous atmospheres, lower friction, lower radio frequency (electrical) and audio (acoustic) noise generation, and very low mechanical time constants are characteristic features that also recommend it for certain applications.

The particular requirements imposed by the intended application of these prototypes (ball bearing test instruments) determined the power rating and the need for elimination of organic outgassing products. Figure 1 illustrates the sealed motor developed on this program. Figure 2 shows the various assemblies which constitute the device.

The dc motor has two elements, one being electro-mechanical (torque-producing) and the other being photo-electronic (commutating).

The torque-producing elements are a two pole permanent magnet rotor, 0.375 in. diameter by 1 in. in length, and a wound stator. The permanent magnet material chosen was highly grain-oriented Alnico V alloy, which has an energy product of 7.5×10^6 gauss-oersteds. The stator is of laminated construction, and uses a high permeability nickel-iron alloy. The armature is a continuous winding in a twelve slot stator, with three terminations.

The photo-optical commutator consists of a tungsten filament lamp, around which rotates a cylindrical sleeve with a slit producing a directional beam. Arranged radially around the rotatable sleeve are six photodiodes which conduct electrical current when illuminated. Power transistors apply the source voltage to the appropriate winding termination when the related photodiode

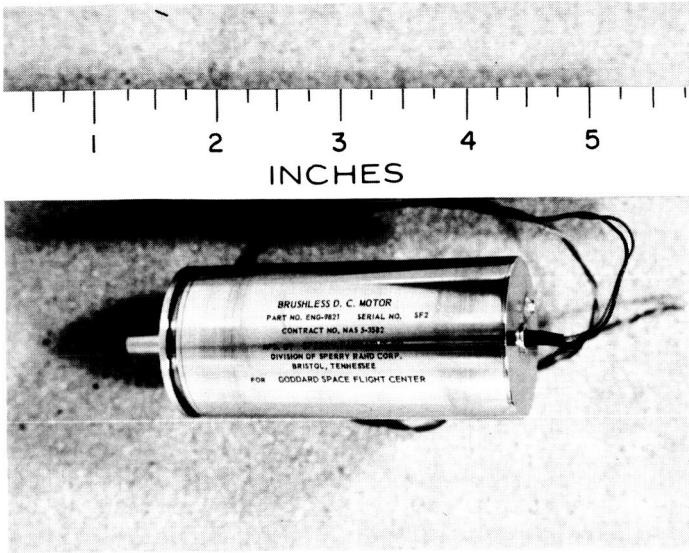


Figure 1—Hermetically sealed 1/2-watt brushless motor.

is illuminated. This tends to keep the imposed field perpendicular to that of the permanent magnet and produces near-maximum torque at all times.

The motors reported in Reference 1, had a peak efficiency of 53% at a power input of 3 watts. Although the basic motor diameter was 1.25 in., the electronic commutator was 2.0 in. in diameter. The total length of the unit was 4.0 in. The nominal operating speed was 3000 rpm to insure good bearing life. All components were safely derated, but no reliability calculations were made.

at a power input of 1 watt and achieve a reliability of 95% (exclusive of bearings) for one year continuous operation. A size reduction to 1.25 in. dia. by 2.75 in. length was required. Other

The objectives of this program were to improve the efficiency to 60% or greater

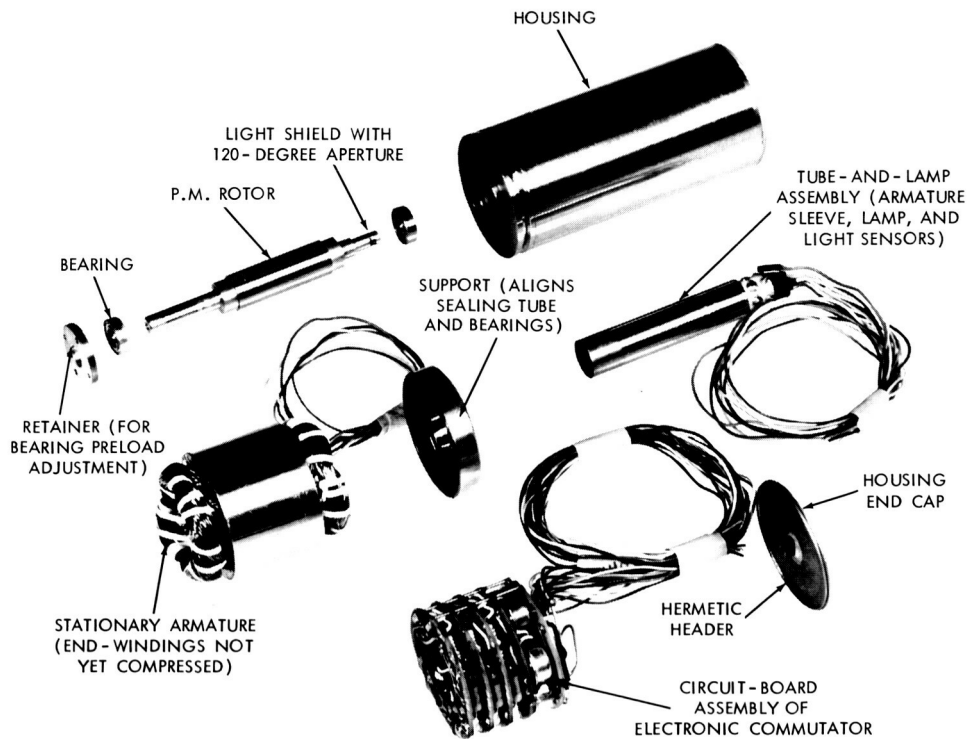


Figure 2—Exploded view of brushless motor.

specific requirements were: hermetic sealing of the windings and electronics to prevent outgassing of organic vapors, the operating speed, and the load. These were imposed by the application of these units for bearing and gear test instrumentation, and bearing torque test data.

The performance characteristics of a typical motor developed on this program are illustrated in Figure 3.

EFFICIENCY

Power losses fall into three categories: fixed, which includes light source power; shunt current and voltage drop in the electronic commutator; rotating, primarily eddy current and hysteresis loss in the magnetic iron of the stator; and copper, due to the I^2R heating in the armature winding.

The *fixed losses* are especially important at low power levels. The power consumed by the light source in the initial prototypes, for example, was 0.3 watt, which was reasonable for a 3 watt motor, but intolerable for a motor with .5 watt total input. Since the silicon photo-detectors have a threshold intensity, and since the luminous efficiency of the light sources varies inversely with the life of the filament; the most direct approach seemed to be to place the detectors closer to the source. This required a smaller diameter lamp, available only in lower voltage ratings. A separate supply for the lamp was ruled out in order to simplify the circuit; and the lamp was placed in series with the motor, using the forward drop of a pair of silicon diodes in parallel with the lamp to limit the lamp voltage to approximately 1.4 volts. Now, however, since the armature switches are open until the detectors are illuminated, it was found necessary to add a shunt circuit which would be non-conducting at normal speed. Additionally, at maximum (no-load) speed, the current through the armature is not normally sufficient to maintain the lamp intensity. A secondary winding was added in order to generate a voltage maintaining the lamp intensity regardless of motor speed and also cut off the starting circuit as the motor speed increased. The power required for the new lamp is approximately .03 watt, a tenfold reduction from the previous design.

The lamp selected for this application, rated at 5.0 volts, is being operated at 1.5 volts, thereby vastly reducing the evaporation rate. The theoretical filament life-to-burnout exceeds 1×10^9 hours (114,000 years). Its mechanical ruggedness is indicated by preliminary vibration tests of a small sample (hard mounted) which recorded no failures at levels up to 70g.

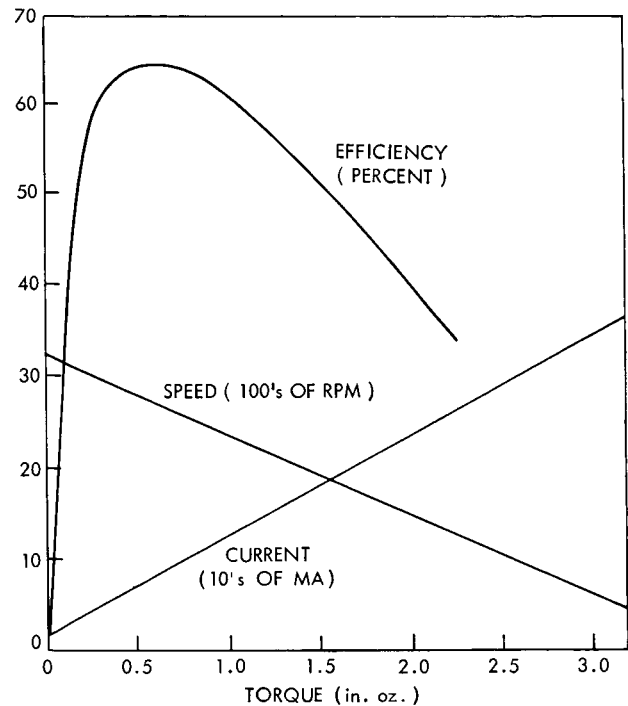


Figure 3—Performance characteristics (24 volt motor).

The *rotational losses* were considerably reduced by changing from a high silicon steel to a nickel-iron alloy and by using thinner laminations.

"*Copper*" losses were reduced by two changes; the first a reduction in the yoke thickness. This and the above-mentioned material change were made possible by a detailed study of the flux

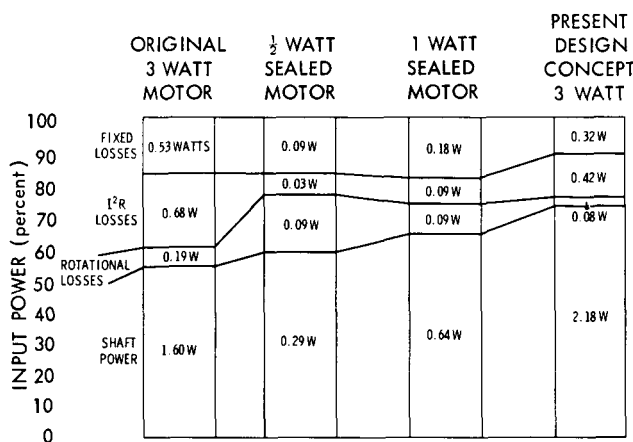


Figure 4—Power breakdown.

level and flux distribution. Secondly, a thin-wall stainless steel case made possible further increase in the slot area by use of a larger diameter lamination.

The effects of the improvements incorporated can best be seen in the chart (Figure 4) which shows the power breakdown for the original motor design, the one-half and one watt motors built on this program, and calculated values for a 3 watt motor incorporating these latest concepts. The chart indicates a forty percent reduction of copper losses. The application of the new design features to the original motor requirement

would increase the efficiency from 53% to 73%. A new circuit concept for the electronic commutator, tested too late to be included in the devices actually fabricated, reduced the voltage drop in the power switches from approximately 1.5 volts to 0.2 volt, yielding an additional five percent improvement.

RELIABILITY

The major reliability improvement resulted from a simplification of the switching circuitry. The motor winding was changed from a six terminal ring winding to a three terminal configuration as shown in Figure 5. Since transistor switches conduct current unidirectionally, two are required at each terminal in either case. Theoretical consideration of the flux distribution and current flow patterns showed that alternate stepping of each of six switches could produce torque with the same smoothness and efficiency as simultaneous commutation of pairs of switches in the ring configuration. The result of this discovery was the reduction, by one-half, of the electronic switching elements required.

The individual elements chosen were analyzed with respect to their operating levels and stresses. Failure rates were assigned based on previous histories and current literature (Reference 2).

The *light source* received special attention since it is a series element in the reliability chain. The voltage dependency of filament life allowed accelerated testing to be adopted. This, combined with fair-sized samples, made possible testing to millions of equivalent unit hours. The lamp initially selected was rejected after testing when the necessary average life was not

achieved. Continued testing of other types showed that lamps of sufficient brilliance could be obtained with sufficient life. The final selection was based on achievement, at a 90% confidence level, of a filament failure rate of less than 1 per 2,000,000 equivalent unit hours of operation. Preliminary vibration tests of short duration up to 70g's uncovered no failures.

The reliability of the *bearings* is a function of bearing speed, lubricant, environment, and external loading. Therefore each application must be analyzed individually. However, for the case where axial preload is the predominant load and fatigue is the anticipated failure mode, a B_{10} life of 500,000 hours was calculated. This leads to a failure rate of 0.15% per 10,000 hours.

The estimated reliability of the *entire motor* for one year operation (8760 hours) as illustrated in Figure 6 is 91.3%. The actual value is somewhat higher since continuous operation would not normally be required of the starting circuit (92.7%) and satisfactory operation for most applications has been demonstrated with one or more of the commutator switches inoperative (94.4%). Hence, a reliability of 93 to 95% depending on the application is predicted for these prototypes.

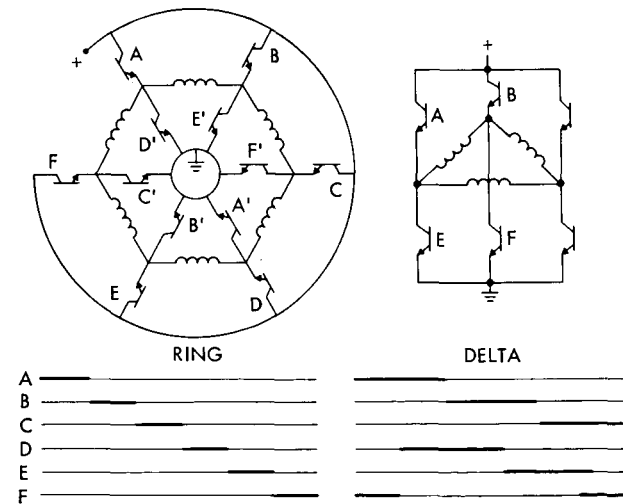


Figure 5—Ring and delta diagrams.

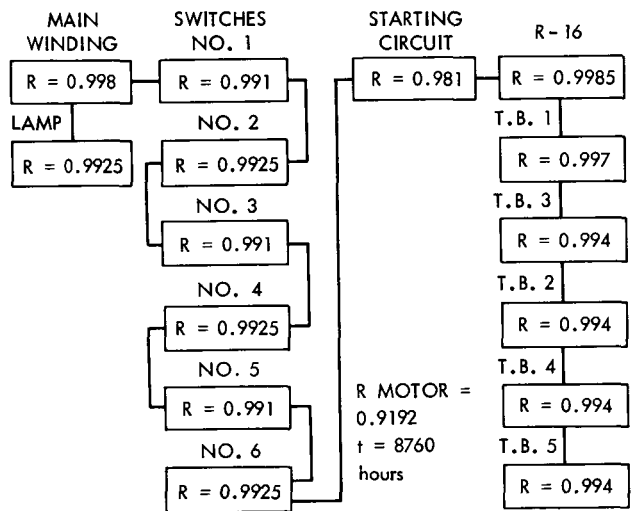


Figure 6—Reliability block diagram.

HERMETIC SEALING

Since these motors were intended for satellite application, outgassing was a design consideration. Organic materials in the motor windings and electronics could contaminate the motor bearings and impair the usefulness of the motor as a test instrument, or adversely affect optical systems in certain applications. The motors were specified to be hermetically sealed to prevent these organic materials from being deposited on the ball bearings; so that the motors might be utilized for bearing test instrumentation in space or in vacuum test chambers. After consideration of the poor space factor* of inorganic insulations and the mechanical problems associated with

*Space factor is a term used to describe the ratio of copper in the windings to the insulating materials in the motor.

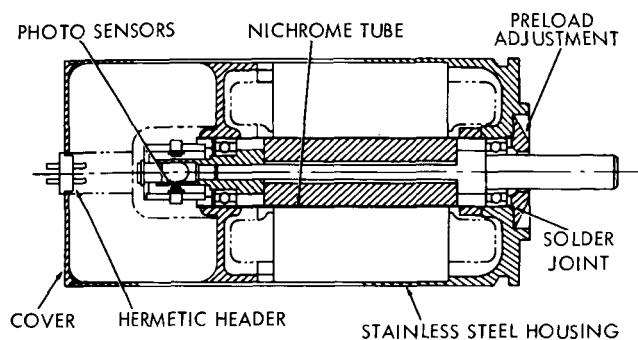


Figure 7—Motor construction detail.

glass or other ceramics in the motor bore, it was decided to utilize a metal tube in the air gap. This construction can be seen in Figure 7.

Experimental work indicated that a tube wall thickness of .005 inch was the minimum practical for stability and handling. The permanent magnet rotor was capable of driving through a considerably larger air gap, therefore, no design change was required. By comparative tests it was found that a high resistivity material of this thickness would not introduce appreciable power loss at the operating speed; therefore, Nichrome was selected. The resultant power loss was .012 watt at 3000 rpm.

The entire stationary portion of the motor is located within a solder sealed metal-ceramic barrier. Only the rotating assembly (i.e., the permanent magnet, shaft, light cup, and bearings) is exposed to the environment.

The glass envelope was sealed with a "solder glass" to a metallic holder which, along with the six photo-sensors, were soldered in the conventional manner to metallized areas on a ceramic cylinder. The differential expansions of these joints were held, by proper choice of materials, to a maximum of 1×10^{-4} in. for the temperature extremes of -10°C to 70°C .

A degradation of light source performance, due to high sealing temperatures, necessitated the use of an epoxy seal substitution which was metallized by vapor deposition on these units. Efforts to return to a completely inorganic seal are being continued for future units.

SIZE REDUCTION

The circuit design which resulted in a reduction by one-half in the number of commutator switches (as previously mentioned) was very helpful in achieving significant size reduction. Also, the photosensors, which were 3/4 in. long and mounted radially in the previous design, required the 2 in. diameter. These photosensors became available in a case less than 1/10-in. long, thus contributing to the size reduction. Efforts to improve the efficiency by reduction of power losses in the commutator made possible the use of micro-packaged solid state components, except for the power switches themselves, which are packaged in "short hat" versions of TO-5 cases.

A size reduction, by a factor of six (to 1.1 cu. in.), was obtained for the electronic commutator. Since this satisfactorily met the design objectives, discrete components on printed circuit boards were used. This choice facilitated testing and utilized devices on which reliability data were available (which would not have been obtainable if integrated circuitry were used).

PERFORMANCE

The characteristics of the two types of motors built during this program are listed below:

Power input	1 watt at 24 vdc
Torque	.25 in.-oz. at 3000 rpm
Stall torque	3.25 in.-oz. at 10 watts
No-load speed	3200 rpm
Power input	1/2 watt at 24 vdc
Torque	.115 in.-oz. at 3000 rpm
Stall torque	2.60 in.-oz. 7.8 watts
No-load speed	3100 rpm

Peak efficiencies as high as 65% are attained at slightly higher-than-rated loads, and the one watt motor is capable of handling continuous stall current of one-half ampere, providing a high available starting torque.

At higher speeds, acceptable for applications where bearing life is adequate, greatly increased power can be obtained from this motor frame size (Figure 8). Although the curve in Figure 8 was calculated, the data has been experimentally verified for a ten-fold increase of power.

CONCLUSION

The state of the art in electronically commutated dc motors has been advanced to a point where no performance or weight penalty remains. Photo-electronic commutation provides a means of improving reliability by eliminating brushes, making the performance of the motor more independent of its environment.

Sealing, to prevent outgassing of organic materials from contaminating adjacent sensitive instruments, was accomplished without significantly affecting performance. The rotating assembly consists only of the main shaft, a permanent magnet rotor, and a light deflector. This inherent simplicity of moving parts make for reliability and the small diameter provides an exceptional torque-to-inertia ratio for fast response.

Since the electronic commutator has built-in power amplification, the control of mechanical output by low-level control signals is possible. Where higher speed operation is feasible from the standpoint of bearing life, more power can be efficiently handled by the same motor size.

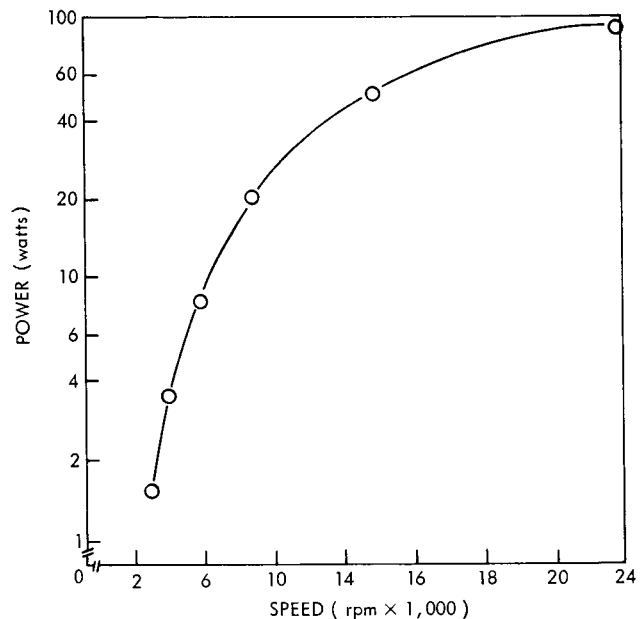


Figure 8—Power output vs. speed.

The techniques have been applied to the area where fixed power losses are very significant, i.e., low power levels. There is no barrier to their application at higher speed and power levels up to the limits of available power transistors. The reliability of the device makes it suitable for applications with stringent environmental and life requirements.

(Manuscript received November 13, 1964)

REFERENCES

1. Studer, P. A., "Development of a Brushless DC Motor for Satellite Application," NASA Technical Note D-2108, February 1964.
2. "Reliability Stress and Failure Rate Data for Electronic Equipment," Military Standardization Handbook 217 (Department of Defense), Washington: U. S. Government Printing Office, 8 August 1962.